J|A|C|S
ARTICLES
Published on Web 01/15/2005

Spectroscopy and Quantum Chemical Modeling Reveal a Predominant Contribution of Excitonic Interactions to the Bathochromic Shift in α-Crustacyanin, the Blue Carotenoprotein in the Carapace of the Lobster *Homarus gammarus*

Arjan A. C. van Wijk,[†] Arnold Spaans,[†] Natallia Uzunbajakava,[‡,#] Cees Otto,[‡] Huub J. M. de Groot,[†] Johan Lugtenburg,[†] and Francesco Buda*[,†]

Contribution from the Leiden Institute of Chemistry, Gorlaeus Laboratories, Leiden University, P.O. Box 9502, NL-2300 RA Leiden, The Netherlands, Faculty of Science and Technology, University of Twente, P.O. Box 217, NL-7500 AE Enschede, The Netherlands

Received August 17, 2004; E-mail: f.buda@chem.leidenuniv.nl

Abstract: To resolve the molecular basis of the coloration mechanism of α-crustacyanin, we used ^{13}C-labeled astaxanthins as chromophores for solid-state ^{13}C NMR and resonance Raman spectroscopy of [6,6′,7,7′]-$^{13}C_4$ α-crustacyanin and [8,8′,9,9′,10,10′,11,11′,20,20′]-$^{13}C_{10}$ α-crustacyanin. We complement the experimental data with time-dependent density functional theory calculations on several models based on the structural information available for β-crustacyanin. The data rule out major changes and strong polarization effects in the ground-state electron density of astaxanthin upon binding to the protein. Conformational changes in the chromophore and hydrogen-bond interactions between the astaxanthin and the protein can account only for about one-third of the total bathochromic shift in α-crustacyanin. The exciton coupling due to the proximity of two astaxanthin chromophores is found to be large, suggesting that aggregation effects in the protein represent the primary source of the color change.

Introduction

Carotenoids are the most widespread class of pigments in both plants and animals. They are responsible for many natural yellow, orange, or red colors. In addition, when carotenoids are associated with proteins, these colors can be modified to green, purple, or blue by the formation of carotenoid−protein complexes. A well-known example of this phenomenon is provided by the lobster *Homarus gammarus*, which is deep blue (λ_{max} 632 nm, aq PO_4 buffer). Heat causes the lobster to change color from blue to red. The high temperature denatures the protein under liberation of the "red" astaxanthin (λ_{max} 472 nm in *n*-hexane, λ_{max} 478 nm in acetone). The bathochromic shift of the astaxanthin chromophore in α-crustacyanin has intrigued scientists for many years.

In a seminal paper, Buchwald and Jencks reported that α-crustacyanin can be irreversibly dissociated in eight β-crustacyanin units.[1] β-Crustacyanin consists of two apoprotein units and two bound astaxanthin units. They also reported the visible, optical rotary dispersion and circular dichroism (CD) spectra of α- and β-crustacyanin. In both systems, the main CD band exhibits a change of sign at the absorption maximum with a negative and a positive peak at wavelengths above and below the absorption maximum, respectively. Renström et al. found that the CD spectra are not influenced by the intrinsic chirality of the astaxanthin in α-crustacyanin.[2] The negative chirality demonstrated by the CD spectra indicates an exciton coupling of the astaxanthins similar to that predicted by exciton theory.[3] Among the possible mechanisms for the perturbed optical properties of astaxanthin in α-crustacyanin, it was also suggested that distortion, such as twisted double bonds induced by the protein, may play a role.[1]

The subsequent resonance Raman (RR) spectroscopy of α-crustacyanin by Carey et al. indicated that the astaxanthin chromophore shows no distortion due to twists in the double bonds of the conjugated system and is in agreement with free relaxed carotenes.[4] On the basis of this resonance Raman study also, the hypothesis of the exciton mechanism was discarded and it was concluded that the bathochromic shift is caused by a charge polarization mechanism possibly induced by charged groups and/or by hydrogen bonds in the binding site.[4]

More recently, to obtain structural information with atomic resolution, a solid-state ^{13}C NMR and resonance Raman spectroscopic study was performed on α-crustacyanin regenerated with astaxanthins that are symmetrically $^{13}C_2$-enriched in

[†] Leiden University.
[‡] University of Twente.
[#] Present address: Philips Research Laboratories, 5656 AA Eindhoven, The Netherlands.

(1) Buchwald, M.; Jencks, W. P. *Biochemistry* **1968**, *7*, 844−859.
(2) Renström, B.; Rönneberg, H.; Borch, G.; Liaaen-Jensen, S. *Comp. Biochem. Physiol., B* **1982**, *71*, 249−252.
(3) Nakanishi, K.; Berova, N. In *Circular Dichroism Principles and Applications*; Nakanishi, K., Berova, N., Woody, R., Eds.; VCH Publishers: New York, 1994; pp 361−398.
(4) Salares, V. R.; Young, N. M.; Beukers, H. J.; Carey, P. R. *Biochim. Biophys. Acta* **1979**, *576*, 176−191.

10.1021/ja045049+ CCC: $30.25

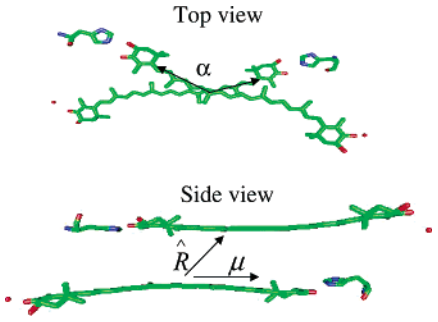

Figure 1. Top view and side view of two astaxanthin molecules in *β*-crustacyanin. α is the angle between the long axes of the astaxanthin molecules; $\hat{R}$ is the unit vector connecting the center of mass of the two molecules, and μ shows the orientation of the transition dipole moment along the axis. The atomic coordinates have been extracted from the Protein Data Bank file (PDB code 1GKA).

the central part.[5−7] The ^{13}C NMR data show substantial downfield shifts of 4.2 and 7.1 ppm for the 14,14′ position and 5.4 and 7.5 ppm for the 12,12′ carbon positions in α-crustacyanin.[5,6] Under the assumption that there is no exciton coupling and together with semiempirical theoretical calculations that fitted the electronic absorption properties, this work led to the hypothesis that there is a strong electrostatic polarization originating from the keto groups, most likely a double protonation.[7] The resonance Raman spectra from the same ^{13}C isotopomers of α-crustacyanin showed that the pattern of the changes in the double bond frequency region differs from that in free astaxanthin itself and all-*E* spheroidene.[7,8]

Recently, the X-ray structure of *β*-crustacyanin at 3.2 Å resolution has been published.[9] The X-ray study showed that in *β*-crustacyanin, two astaxanthins are present in parallel planes that cross at a distance of 7 Å, just a little outside the centers of the chromophores, as shown in Figure 1. The vectors of the central axis are oriented at 120°. The conformation around the 6−7 and 6′−7′ bonds is planar s-trans, in contrast to free astaxanthin, which has an s-cis conformation. The oxygen at the 4′-keto group is close to His-90 and His-92 for astaxanthin 1 and 2, respectively. The two other keto groups have interactions with Asp, two Tyr residues, a Ser, and a bound water molecule. Although the increased conjugation due to the end ring's coplanarization should lead to a bathochromic shift with respect to free astaxanthin, it has been stated that this effect is not sufficient to explain the color of *β*-crustacyanin.[9]

Despite considerable progress made in structural and spectroscopic studies, a clear converging picture on the dominant mechanism for the bathochromic shift in crustacyanin is still missing. There are two main hypotheses that are still debated: (i) the "on-site" (intramolecular) mechanism involving protein-induced conformational changes and/or charge-polarization effects modifying the electronic ground state of the chromophore; and (ii) the aggregation (intermolecular) mechanism due to the interaction of the chromophores in the subunits of crustacyanin inducing an exciton coupling of the transition dipole moments in the excited state.

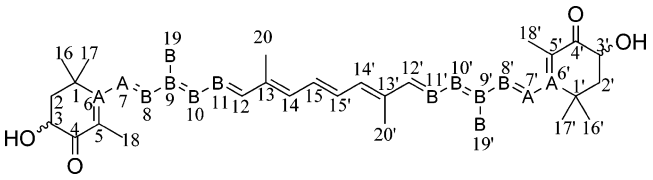

Figure 2. Molecular structure and IUPAC numbering of synthetic all-*E* astaxanthin (3,3′-didehydro-*β*,*β*-carotene-4,4′-dione) as a mixture of 25% (3*R*,3′*R*), 25% (3*S*,3′*S*), and 50% (3*R*,3′*S*). A is the ^{13}C for [6,6′,7,7′]-$^{13}C_4$-all-*E* astaxanthin (**2a**). B is the ^{13}C for [8,8′,9,9′,10,10′,11,11′,19,19′]-$^{13}C_{10}$-all-*E* astaxanthin (**2b**).

To resolve the precise molecular basis of the coloration mechanism of α-crustacyanin, we used ^{13}C-labeled astaxanthins as chromophores for solid-state ^{13}C NMR and resonance Raman spectroscopy of [6,6′,7,7′]-$^{13}C_4$ α-crustacyanin (**1a**) and [8,8′,9,9′,10,10′,11,11′,19,19′]-$^{13}C_{10}$ α-crustacyanin (**1b**), establishing the electronic charge distribution and vibrational contribution of the remaining sp^2 carbon atoms. Figure 2 shows the structure and numbering of the all-*E* astaxanthin (3,3′-didehydro-*β*,*β*-carotene-4,4′-dione) chromophore. The position of the ^{13}C enrichment is marked with (A) for [6,6′,7,7′]-$^{13}C_4$ astaxanthin (**2a**) and with (B) for [8,8′,9,9′,10,10′,11,11′,19,19′]-$^{13}C_{10}$ astaxanthin (**2b**).

We complement the spectroscopic data with quantum mechanical calculations of the electronic ground state and excitation energies of various astaxanthin models based on the structural information available for *β*-crustacyanin. The theoretical investigation is crucial to identifying the relative importance of different mechanisms that may contribute to the total bathochromic shift.

Materials and Methods

Synthesis of ^{13}C-Labeled Astaxanthins. The synthetic strategy for preparing astaxanthin with 99% ^{13}C enrichment at any position or combination of positions has been reported earlier by our group.[10] For the ^{13}C enrichment of the 6,6′,7,7′-position, the commercially available $^{13}C_2$-acetonitrile was used. The ^{13}C incorporation at the 8,8′,9,9′,10,10′,11,11′,19,19′ positions was effected by $^{13}C_5$-triethyl-3-methyl-4-phosphonocrotonate, which was prepared analogous to the corresponding nitrile derivative which was used earlier in our group for the synthesis of uniformly ^{13}C-enriched retinal.[11]

A quantity of 140 mg (0.23 mmol) of all-*E* [6,6′,7,7′]-$^{13}C_4$ astaxanthin (**2a**) (25% (3*R*,3′*R*), 25% (3*S*,3′*S*), and 50% (3*R*,3′*S*)) was obtained in 10 steps starting from 1.3 g (30.7 mmol) $^{13}C_2$-acetonitrile. Similarly, 50 mg (0.08 mmol) of all-*E* [8,8′,9,9′,10,10′,11,11′,19,19′]-$^{13}C_{10}$ astaxanthin (**2b**) (25% (3*R*,3′*R*), 25% (3*S*,3′*S*), and 50% (3*R*,3′*S*)) was obtained. We recorded solution ^{1}H and ^{13}C NMR spectra of **2a** and **2b** and compared them with the spectra of unlabeled astaxanthin to observe the effect of the specific ^{13}C enrichment on the NMR spectra and to verify the position and level of the ^{13}C enrichment. NMR spectroscopy confirmed the purity of the all-*E* [6,6′,7,7′]-$^{13}C_4$ astaxanthin **2a** and [8,8′,9,9′,10,10′,11,11′,19,19′]-$^{13}C_{10}$ astaxanthin **2b** and >99% ^{13}C enrichment at the desired positions. The NMR data are available as Supporting Information.

Isolation and Reconstitution of α-Crustacyanin. The blue protein α-crustacyanin was extracted from lobster carapace and subsequently purified by anion-exchange and gel-filtration chromatography according

(5) Weesie, R. J.; Askin, D.; Jansen, F. J. H. M.; de Groot, H. J. M.; Lugtenburg, J.; Britton, G. *FEBS Lett.* **1995**, *362*, 34−38.
(6) Weesie, R. J.; Jansen, F. J. H. M.; Merlin, J. C.; Lugtenburg, J.; Britton, G.; de Groot, H. J. M. *Biochemistry* **1997**, *36*, 7288−7296.
(7) Weesie, R. J.; Merlin, J. C.; de Groot, H. J. M.; Britton, G.; Lugtenburg, J.; Jansen, F. J. H. M.; Cornard, J. P. *Biospectroscopy* **1999**, *5*, 358−370.
(8) Dokter, A. M.; van Hemert, M. C.; In't Velt, C. M.; van der Hoef, K.; Lugtenburg, J.; Frank, H. A.; Groenen, E. J. J. *J. Phys. Chem. A* **2002**, *106*, 9463−9469.
(9) Cianci, M.; Rizkallah, P. J.; Olczak, A.; Raferty, J.; Chayen, N. E.; Zagalsky, P. F.; Helliwel, J. R. *Proc. Natl. Acad. Sci. U.S.A.* **2002**, *99*, 9795−9811.
(10) Jansen, F. J. H. M.; Lugtenburg, J. *Eur. J. Org. Chem.* **2000**, 829−836.
(11) Creemers, A. F. L.; Lugtenburg, J. *J. Am. Chem. Soc.* **2002**, *124*, 6324−6334.

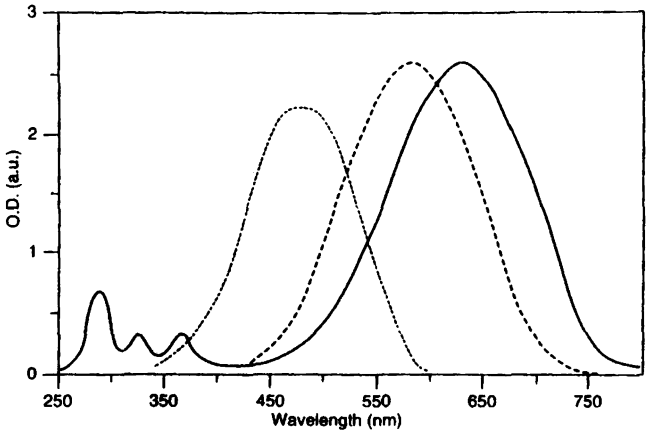

Figure 3. UV−vis absorption spectra of astaxanthin in dimethylformamide (· · ·), β-crustacyanin in aq PO_4 buffer (- - -), and α-crustacyanin in aq PO_4 buffer (—) (from Britton et al.[13]).

to the procedure described by Zagalsky.[12] The purity of α-crustacyanin was determined by the ratio of absorbance at 632 and 280 nm, and fractions with A_{632}:A_{280} > 3.5 were used for reconstitution. The total amount of α-crustacyanin was determined from the absorbance at 632 nm. A molar extinction coefficient, $\epsilon = 1.25 \times 10^5$ M^{-1} cm^{-1}, was used. The UV−vis spectra of astaxanthin, α-crustacyanin, and β-crustacyanin are shown in Figure 3.

The reconstitution procedure was based on the method described by Zagalsky.[12] Briefly, astaxanthin was removed from the carotenoprotein with acetone/ether extraction. To the resulting colorless apoprotein was quickly added the labeled carotenoid (**2a** or **2b**) in acetone; the mixture was stirred, and phosphate buffer was added. The color of the complex quickly turned blue-purple. The mixture was dialyzed overnight against 5 L phosphate buffer, pH 7.0, and the reconstituted complex was purified on a short gel-filtration column; the purity was determined by the A_{632}:A_{280} ratio with UV−vis spectroscopy. This method yielded [6,6′,7,7′]-$^{13}C_4$ α-crustacyanin (**1a**) and [8,8′,9,9′,10,10′,11,11′,19,19′]-$^{13}C_{10}$ α-crustacyanin (**1b**).

Solution NMR Spectroscopy. ^{1}H NMR spectra, ^{1}H−^{13}C-decoupled NMR spectra, and ^{13}C NMR spectra of astaxanthin in $CDCl_3$ were recorded on a Bruker AM-600 spectrometer using tetramethylsilane (^{1}H $\delta = 0$ ppm) or $CDCl_3$ (^{13}C $\delta = 77.00$ pm) as internal standard.

Solid-State NMR Spectroscopy. Approximately 10 mg of α-crustacyanin reconstituted with ^{13}C-labeled astaxanthin was used for each SSNMR sample. The solutions were first concentrated with a 100 kDa Macrosep centrifugal concentrator to a volume of 2 mL. Subsequently, 10 kDa Eppendorf centrifugal concentrators were used to reduce the volume to 200 μL. The resulting very dense blue solutions were transferred to a 4 mm MAS rotor with a homemade centrifugal swing-out device. NMR spectra were recorded at 188 MHz ^{13}C frequency using a Bruker DSX-750 spectrometer equipped with a double-resonance MAS probe. The samples were cooled to 223 K, and the MAS spin rate was 12 kHz for all experiments. The CP/MAS spectra were recorded using 2.0 ms ramped cross-polarization and two-pulse phase modulation decoupling during acquisition.[14,15] Radio frequency-driven (RFDR) dipolar recoupling correlation spectra were acquired using a pathway-selective phase-cycling method.[16] The 2D heteronuclear correlation (HETCOR) spectra were recorded with phase-modulated Lee−Goldburg decoupling during the t_1 period.[17,18]

Resonance Raman Spectroscopy. A home-built confocal Raman microspectrometer was used to measure Raman spectra of the carotenoids (dissolved in $CHCl_3$) and carotenoproteins (dissolved in aqueous phosphate buffer). A Kr ion laser (Coherent Innova 90-K) with an emission wavelength of 647.1 nm was used to excite the Raman scattering. The laser power on the sample was 5 mW. A dichroic beam splitter (660 DCLP, Chroma Technology Corp.) was used in order to separate the Raman scattered light from the laser light, which was further suppressed by a holographic notch filter (Kaiser Optical Systems Inc.) with an optical density of 4.0 at the excitation wavelength.

The measurement time per spectrum was 50 s. The spectrograph stage (Jobin-Yvon HR460) was equipped with a blazed holographic grating with 1200 l/mm. This resulted in a dispersion of 0.8 cm/pixel on a CCD camera (Roper Scientific, Inc.). This camera contains a liquid-nitrogen-cooled, back-illuminated chip with 1100 × 330 pixels and a pixel size of 24 × 24 μm^2. The setup is connected to a computer that controls the instrument settings, the data read-out, and the data storage.

Computational Methods and Details. The geometry optimization of astaxanthin and of the various models considered here was performed with the semiempirical AM1 method. The calculation of excitation energies and transition dipole moments to the optically allowed ^1B_u excited state was performed using time-dependent density functional theory (TDDFT).[19] We used the BLYP generalized gradient approximations for the exchange and correlation functional.[20] The calculations were done with a triple-ζ Slater-type orbital (STO) basis set with a single set of polarization functions using the Amsterdam Density Functional (ADF) package.[21]

TDDFT allows calculating properties, such as excitation energies, through the linear density response of the system to the external time-dependent field. It is known that TDDFT shows a systematic underestimation of the excitation to the optically allowed ^1B_u state in linear polyenes by about 0.5−0.7 eV.[22] However, the general trend of decreasing excitation energy with chain length is correctly reproduced. Since here we are interested in the bathochromic shift of the absorption energy rather than in the absolute values, TDDFT represents a good compromise between accuracy and computational efficiency for our models. Indeed, the use of more accurate multiconfiguration self-consistent field (MCSCF) calculations would be computationally prohibitive for the large molecules studied here.

The aggregation effects are estimated using a simple dipole−dipole approximation of the interaction between the two astaxanthins in the geometry of the β-crustacyanin dimer. Within this approximation, the interaction that gives an estimate of the exciton splitting can be written as

$$V_{12} = \frac{1}{4\pi\epsilon_0}\frac{\mu_1\mu_2 - 3(\mu_1\hat{R})(\mu_2\hat{R})}{R^3}$$

Here, μ is the transition dipole moment; $\hat{R}$ is the unit vector connecting the two molecules, and R is the distance between the two molecules. The transition dipole moment is obtained from the TDDFT calculation, and the orientation factor is estimated using the β-crustacyanin structure. We used the dielectric constant in the vacuum, though inside the protein, it may generally be larger.

(12) Zagalsky, P. F. *Methods Enzymol.* **1985**, *111B*, 216−247.
(13) Britton, G.; Weesie, R. J.; Askin, D.; Warburton, J. D.; Gallardo-Guerrero, L.; Jansen, F. J. H. M.; de Groot, H. J. M.; Lugtenburg, J.; Cornard, J. P.; Merlin, J. C. *Pure Appl. Chem.* **1997**, *69*, 2075−2085.
(14) Pines, A.; Gibby, M. G.; Waugh, J. S. *J. Chem. Phys.* **1973**, *59*, 569−573.
(15) Balaban, T. S.; Holzwarth, A. R.; Schaffner, K.; Boender, G. J.; de Groot, H. J. M. *Biochemistry* **1995**, *34*, 15259−15266.
(16) Boender, G. J.; Raap, J.; Prytulla, S.; Oschkinat, H.; de Groot, H. J. M. *Chem. Phys. Lett.* **1995**, *237*, 502−508.
(17) van Rossum, B. J.; Boender, G. J.; de Groot, H. J. M. *J. Magn. Reson. A* **1996**, *120*, 274−277.
(18) Vinogradov, E.; Madhu, P. K.; Vega, S. *Chem. Phys. Lett.* **1999**, *314*, 443−450.
(19) Gross, E. K. U.; Kohn, W. *Adv. Quantum Chem.* **1990**, *21*, 255. (b) Casida, M. E. In *Recent Developments and Applications of Modern Density Functional Theory*; Seminario, J. M., Ed.; Elsevier: Amsterdam, 1996.
(20) Becke, A. D. *J. Chem. Phys.* **1986**, *84*, 4524. (b) Lee, C.; Yang, W.; Parr, R. *Phys. Rev. B* **1998**, *37*, 785.
(21) Fonseca Guerra, C.; Snijders, J. G.; te Velde, G.; Baerends, E. J. *Theor. Chem. Acc.* **1998**, *99*, 391. (b) van Gisbergen, S. J. A.; Snijders, J. G.; Baerends, E. J. *J. Comput. Phys. Commun.* **1999**, *118*, 119.
(22) Hsu, C.; Hirata, S.; Head-Gordon, M. *J. Phys. Chem. A* **2001**, *105*, 451−458.

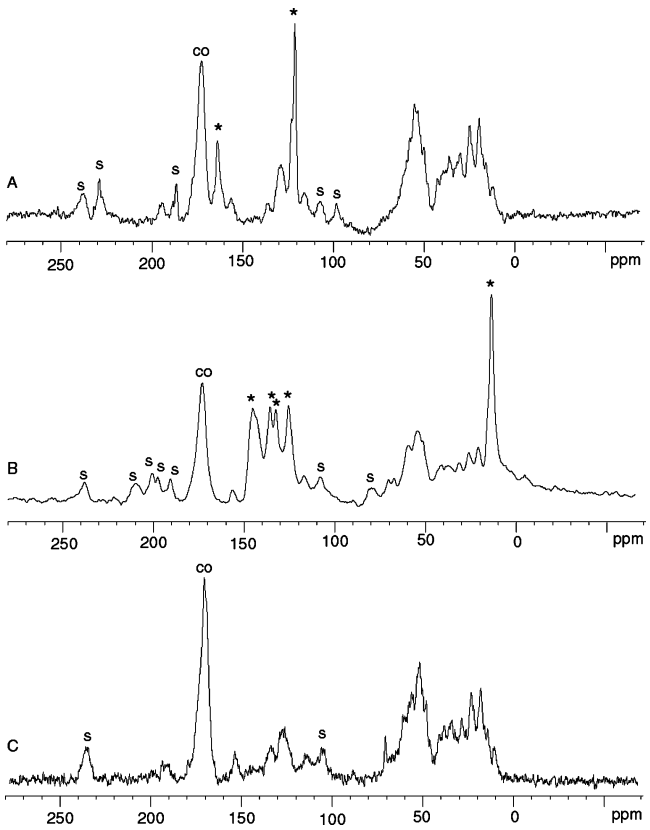

Figure 4. ^{13}C CP/MAS NMR spectra of α-crustacyanin: A, reconstituted with [6,6′,7,7′]-$^{13}C_4$ astaxanthin (**1a**); B, reconstituted with [8,8′,9,9′, 10,10′,11,11′,19,19′]-$^{13}C_{10}$ astaxanthin (**1b**), and the natural abundance spectrum (C). The signals arising from the ^{13}C enrichment are indicated with (∗). The spinning sidebands are marked with (s). The signal arising from the carbonyl carbons of the protein is marked with (CO). The spectra are recorded at 188 MHz ^{13}C frequency and 223 K with a MAS spin rate of 12 kHz.

Results

Solid-State NMR Spectroscopy of α-Crustacyanin. ^{13}C CP/MAS NMR data were collected from natural abundance α-crustacyanin, [6,6′,7,7′]-$^{13}C_4$ α-crustacyanin (**1a**), and [8,8′,9,9′, 10,10′,11,11′,19,19′]-$^{13}C_{10}$ α-crustacyanin (**1b**) (Figure 4). The natural abundance spectrum of α-crustacyanin shows the characteristic features of a protein spectrum. Between 0 and 40 ppm, the signals of the aliphatic side chains of the amino acids are observed. Around 50 ppm, the resonances from C_α atoms are found, while around 120 ppm, the responses of the aromatic amino acid residues are recognized. The sharp signal at 170 ppm is assigned to the carbonyl−carbon of the peptide bonds.

In the spectra of Figure 4, the signals marked with (*) are not detected for the natural abundance sample and arise from the ^{13}C labels of the chromophore. The signal at 120 ppm in Figure 4A is assigned to the ^{13}C label at C7/C7′ of the chromophore since the shift is comparable with δ(C7) = 123.3 ppm observed for astaxanthin in $CDCl_3$.[23] The signal from the ^{13}C label at C6/C6′ of the chromophore at 162 ppm is also close to δ(C6) = 162.4 ppm for the C6 of free astaxanthin in $CDCl_3$. The NMR response appears symmetric as no difference between C6 and C6′ and between C7 and C7′ was observed within the resolution of the NMR spectra.

(23) Englert, G.; Kienzle, F.; Noack, K. *Helv. Chim. Acta* **1977**, *60*, 1209.

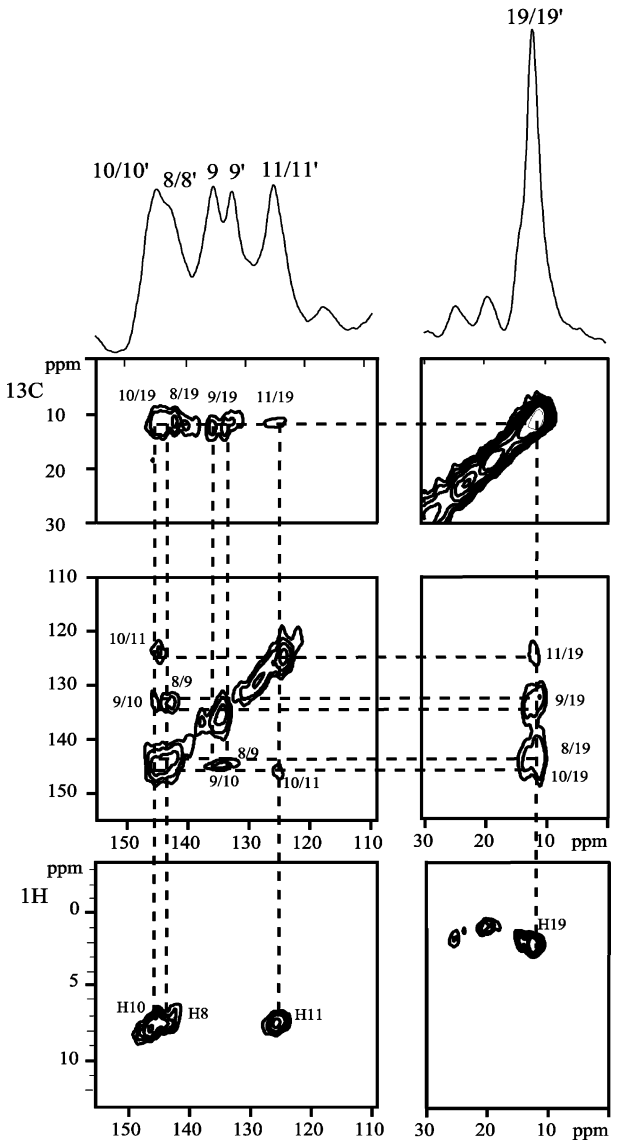

Figure 5. Contour region of the 2D homonuclear (^{13}C−^{13}C) and 2D heteronuclear (^{1}H−^{13}C) dipolar correlation spectra of [8,8′,9,9′,10,10′, 11,11′,19,19′]-$^{13}C_{10}$ crustacyanin (**1b**). The ^{13}C−^{13}C correlations and ^{13}C−^{1}H correlations are shown.

In the spectrum of **1b**, the strongest signal is at 11 ppm, which is assigned to C19/C19′ (Figure 4B). This shift is close to the shift of C19/C19′ in solution (δ(C19) = 12.6 ppm in $CDCl_3$).[23] The signals between 120 and 150 ppm from the C8−C11 can be assigned using 2D homonuclear (^{13}C−^{13}C) and 2D heteronuclear (^{1}H−^{13}C) dipolar correlation techniques. Figure 5 shows the contour region of the 2D RFDR and 2D HETCOR NMR spectra of [8,8′,9,9′,10,10′,11,11′,19,19′]-$^{13}C_{10}$ α-crustacyanin. Starting from the signal of C19/C19′, we assigned the label clusters. The signal of C11/C11′ was found at 123 ppm, similar to the value in solution (δ(C11) = 124.1 ppm in $CDCl_3$).[23] A correlation between C11 and C10 was found, and the C10/C10′ chemical shift was determined at 144 ppm. This value is about 9 ppm higher compared to the value in solution (δ(C10) = 135.1 ppm in $CDCl_3$).[23] From C10, correlations to C8 and C9 were found at 142, 134, and 131 ppm. The signals at 134 and 131 ppm show no correlation in the HETCOR spectrum and are assigned to C9 and C9′, respectively. These values are comparable to the chemical shift of C9 for astaxanthin in solution

Table 1. ^{13}C NMR Data of Astaxanthin in Solution and Astaxanthin Bound in α-Crustacyanin

C atom	$\delta_{solution}$[a]	$\delta_{\alpha-crustacyanin}$[b]	$\Delta_{binding}$
4/4′	200.4	203.4	3.0
6/6′	162.4	162	0
7/7′	123.3	120	−3
8/8′	142.2	142	0
9/9′	134.7	133.8, 130.5	−0.9, −4.2
10/10′	135.1	144	9
11/11′	124.1	123	−1
12/12′	139.7	145.1, 147.2	5.4, 7.5
13/13′	136.7	135.2	−1.5
14/14′	133.8	138.0, 140.9	4.2, 7.1
15/15′	130.7	129.5	−1.2
19/19′	12.6	11.1	−1.5
20/20′	12.8	11.1	−1.7

[a] Data from Englert et al. (ref 23). [b] Data of C4/4′, C12/12′, C13/13′, C14/14′, C15/15′, and C20/20′ from Britton et al. (ref 13).

(δ(C9) = 134.7 ppm in $CDCl_3$).[23] Finally, the signal at 142 ppm was assigned to C8/C8′. Again, this signal is comparable to the value for astaxanthin in solution (δ(C8) = 142.2 ppm in $CDCl_3$).[23] Table 1 gives the ^{13}C NMR data of astaxanthin in α-crustacyanin and the comparison with the free carotenoid in $CDCl_3$.

From the NMR data, we could not discriminate between C8/C8′, C10/C10′, C11/C11′, and C19/C19′, which shows that for these carbon sites, the interactions of the chromophore with the protein on both halves of the astaxanthin are similar. Only for C9/C9′, C12/C12′, and C14/14′ are slightly different chemical shifts observed, confirming that the binding of the chromophore is not fully symmetrical.[6] The slight asymmetry is probably caused by a difference in protein environment, although it is not clear why these specific signals can be resolved as distinct signals, whereas the signals of other pairs overlap.

We found that only minor changes in the ground-state electron density of the C atoms 8−11 of astaxanthin occur upon binding. In particular, small shifts to higher field are found for C7/C7′ (−3 ppm) and C9/C9′(−1/−4 ppm), and a relatively large downfield shift is detected for C10/C10′ (+9 ppm). The small effect for the C8 effectively rules out the hypothesis of a polarization originating from the keto groups of the chromophore. NMR studies on protonated canthaxanthin show that a strong electrostatic effect, like a single or double protonation, should give increasingly larger changes in the chemical shift values of the even-numbered atoms closer to the ring,[24] in contrast with our data.

Resonance Raman Characterization of ^{13}C-Labeled Astaxanthin. The resonance Raman spectra of astaxanthin, [6,6′,7,7′]-$^{13}C_4$ astaxanthin (**2a**), and [8,8′,9,9′,10,10′,11,11′,19,19′]-$^{13}C_{10}$ astaxanthin (**2b**) are shown in Figure 6. The spectra of β,β-carotene and [12,12′,13,13′,14,14′,15,15′,20,20′]-$^{13}C_{10}$ β,β-carotene are added for comparison.

The RR spectrum of unlabeled astaxanthin (Figure 6C) is characterized by three main lines at 1520 (ν_1), 1158 (ν_2), and 1005 cm^{-1} (ν_3), in agreement with data for all-*E* astaxanthin published before by other groups.[25,26] The intense line around 1520 cm^{-1} has been assigned to the C=C stretch vibrations of the central part of the polyene chain. The line of astaxanthin at 1158 cm^{-1} has been assigned previously to a combination of the unmethylated C−C stretch and the C−H in plane-bending vibrations. The ν_3-line at 1005 cm^{-1} is relatively weak compared to the ν_1 and ν_2 signals and is assigned to the CH_3 in-plane rocking vibrations.

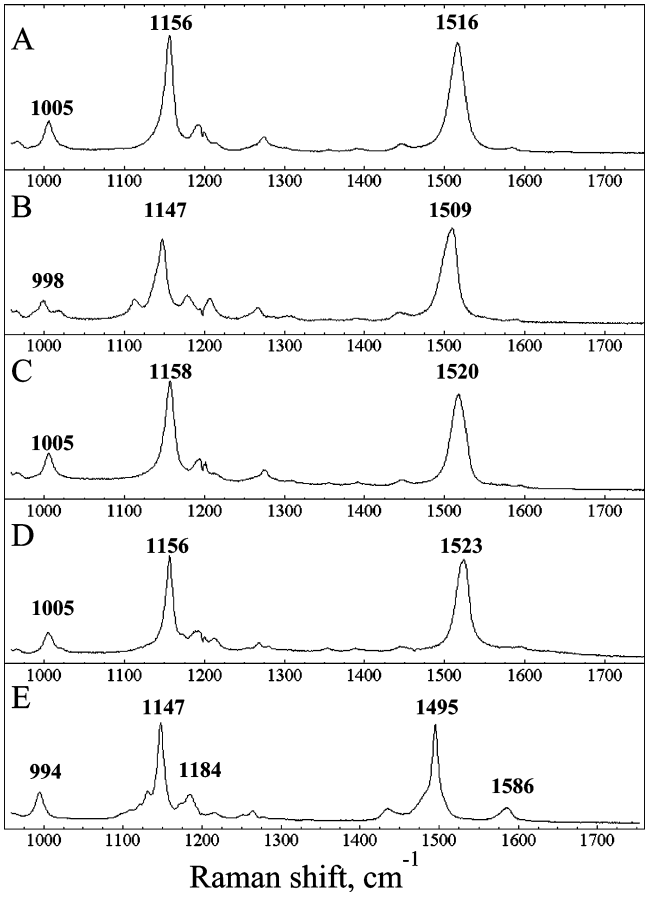

Figure 6. Resonance Raman spectra: (A) [6,6′,7,7′]-$^{13}C_4$ astaxanthin (**2a**); (B) [8,8′,9,9′,10,10′,11,11′,19,19′]-$^{13}C_{10}$ astaxanthin (**2b**); (C) natural abundance astaxanthin; (D) β,β-carotene; and (E) [12,12′,13,13′,14,14′,15,15′,20,20′]-$^{13}C_{10}$ β,β-carotene.

The RR spectra of $^{13}C_4$ astaxanthin (**2a**, see Figure 6A) and $^{13}C_{10}$ astaxanthin (**2b**, see Figure 6B) were compared with the spectrum of natural abundance astaxanthin (Figure 6C) to study the effect of the ^{13}C labeling. The spectrum of [6,6′,7,7′]-$^{13}C_4$ astaxanthin (**2a**) is almost identical to the spectrum of unlabeled astaxanthin, with the main lines at 1516, 1156, and 1005 cm^{-1}. The ^{13}C labels are at the end of the central polyene chain and have little or no effect on the RR spectrum.

The bands of [8,8′,9,9′,10,10′,11,11′,19,19′]-$^{13}C_{10}$ astaxanthin (**2b**, see Figure 6B) are shifted compared to those of unlabeled astaxanthin. Although the shape and relative intensities of the lines are similar, a significant shift to lower frequencies is observed for the main lines. The ν_1-line is shifted to 1509 cm^{-1} (−11 cm^{-1}); the ν_2-line is shifted to 1147 cm^{-1} (−11 cm^{-1}), and the ν_3-line is shifted by −7 cm^{-1} from 1005 to 998 cm^{-1}. Moreover, the ^{13}C isotope substitution leads to a more complex band pattern near the ν_2-line, where a band is observed at 1115 cm^{-1}, and the weak band of astaxanthin around 1200 cm^{-1} is split into bands at 1185 and 1205 cm^{-1}.

The RR spectrum of β,β-carotene (see Figure 6D) is very similar to the spectrum of astaxanthin, though the end groups are different.[8] The spectrum of $^{13}C_{10}$ β,β-carotene (Figure 6E),

(24) Kjeldahl-Andersen, G.; Lutnaes, B. F.; Liaaen-Jensen, S. *Org. Biomol. Chem.* **2004**, *2*, 489−498.
(25) Weesie, R. J.; Merlin, J. C.; Lugtenburg, J.; Britton, G.; Jansen, F. J. H. M.; Cornard, J. P. *Biospectroscopy* **1999**, *5*, 19−33.
(26) Merlin, J. C. *Pure Appl. Chem.* **1985**, *57*, 785−792.

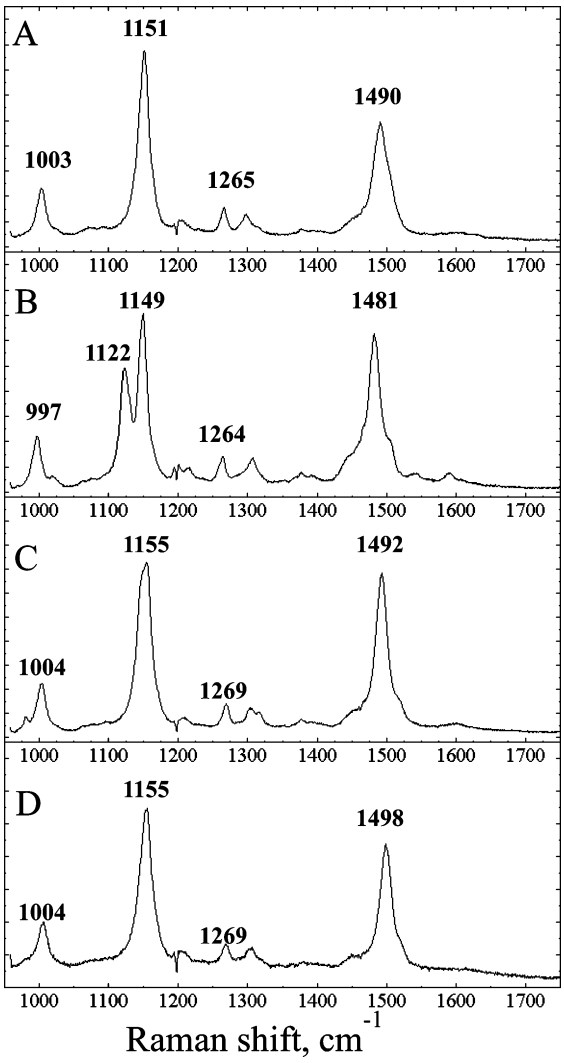

Figure 7. Resonance Raman spectra: (A) α-crustacyanin reconstituted with [6,6′,7,7′]-$^{13}C_4$ astaxanthin (**1a**); (B) α-crustacyanin reconstituted with [8,8′,9,9′,10,10′,11,11′,19,19′]-$^{13}C_{10}$ astaxanthin (**1b**); (C) natural abundance α-crustacyanin; and (D) natural abundance *β*-crustacyanin.

with ^{13}C labels in the central part of the polyene chain, is clearly different from the spectrum of unlabeled *β*,*β*-carotene, with shifts of the ν_1-line (-28 cm^{-1}), ν_2-line (-9 cm^{-1}), and ν_3-line (-11 cm^{-1}). The ^{13}C isotope substitution in *β*,*β*-carotene also leads to more complex spectral features around the ν_2 band, and a Raman band at 1125 cm^{-1} can be observed as a shoulder. In addition, the intensity of the broad line at 1586 cm^{-1} is increased, and small changes in the fingerprint region are observed. This confirms that ^{13}C labeling in the central parts of carotenoids significantly changes the RR spectra.

Resonance Raman Characterization of α-Crustacyanin. The resonance Raman spectra of α-crustacyanin, $^{13}C_4$ α-crustacyanin (**1a**), and $^{13}C_{10}$ α-crustacyanin (**1b**) are shown in Figure 7. The spectrum of α-crustacyanin (see Figure 7C) is distinctly different from the spectra of astaxanthin. The ν_1-line is shifted from 1520 to 1492 cm^{-1}, a shift which is correlated with the change in absorption maximum from ∼472 to 632 nm, qualitatively following the empirical relationship between ν_1 and $1/\lambda_{max}$.[27,28] In the fingerprint region between 1250 and 1400 cm^{-1}, new Raman bands appear that are absent in free astaxanthin. The vibrations of the ν_2 and ν_3-line do not shift upon binding, although small shoulders appear on these bands.

The spectrum of $^{13}C_4$ α-crustacyanin (Figure 7A) is similar to the spectrum of natural abundance α-crustacyanin. Only minor shifts of the ν_1-line (1490 cm^{-1}), the ν_2-line (1151 cm^{-1}), and the ν_3-line (1003 cm^{-1}) are observed, compared to those of the natural abundance α-crustacyanin.

However, the spectrum of $^{13}C_{10}$ α-crustacyanin (see Figure 7B) shows distinct differences compared to that of natural abundance α-crustacyanin. The ν_1-line shows a downshift of 11 cm^{-1}, from 1492 cm^{-1} in natural abundance astaxanthin to 1481 cm^{-1} in **1b**. The ν_2-line in α-crustacyanin is shifted -6 cm^{-1} to 1149 cm^{-1} and is broadened. The broadening is related to a protein-induced splitting in otherwise degenerate vibrational modes. The ^{13}C isotope labeling in α-crustacyanin demonstrates a complete lifting of the degeneracy as an intense band arises next to the ν_2 band at 1122 cm^{-1}. The ν_3-line shifts from 1005 to 997 cm^{-1} due to ^{13}C labels in **1b**.

For comparison, we also recorded the spectrum of *β*-crustacyanin, which is shown in Figure 7D. The band positions of the ν_2-line and ν_3-line are the same as those for the α-crustacyanin, although the broadening of the ν_2-line is smaller for *β*-crustacyanin than for α-crustacyanin. The ν_1-line is shifted to 1498 cm^{-1}, which is in line with the λ_{max} (586 nm) of *β*-crustacyanin being smaller than for α-crustacyanin (632 nm).[27] This indicates that the interactions of the chromophore with the protein are similar in α- and *β*-crustacyanin.

Models and Quantum Chemical Calculations. To analyze the relative importance of the possible mechanisms contributing to the total bathochromic shift, we have considered the following models: (I) free astaxanthin, (II) 6-s-*trans*-astaxanthin with the end rings coplanar to the polyene chain, and (III) 6-s-*trans*-astaxanthin, including a hydrogen-bonded histidine analogue (methylimidazole) and a water molecule according to the X-ray data on *β*-crustacyanin.[9] Comparison of model I and model II gives a measure of the shift induced by the increased conjugation due to the ring coplanarization. Model III shows the importance of the polarization effects due to the hydrogen bonding with the keto oxygens.

In Table 2, we report the first excitation energy with a considerable oscillator strength obtained with TDDFT for the three carotenoid models described above. This excitation corresponds to the allowed ^1B_u -like excited state and can be described to a large extent as a HOMO to LUMO transition (contributing to more than 80% of the excitation) in all cases. To compare the shift in nanometers with the experimental values, we have also reported in the second column a set of values shifted by 0.7 eV. With this offset, the excitation energy

Table 2. Excitation Energies for Carotenoid Models I, II, and III Obtained with TDDFT[a]

model	Δ*E* (eV)	Δ*E* (eV) + 0.7 eV shift
I (s-*cis*-astaxanthin)	1.89	2.59 (478 nm)
II (s-*trans*-astaxanthin)	1.77	2.47 (502 nm)
III (s-*trans*-astaxanthin + water + His)	1.70	2.40 (517 nm)
III + exciton splitting		1.91 (650 nm)

[a] In the second column, we have shifted the TDDFT results for a comparison with the experimental data (see text). In parentheses, we give the corresponding λ_{max} in nanometers. The excitation energy in the last row is obtained by adding the estimated exciton splitting to the TDDFT result of model III.

(27) Merlin, J. C. *Raman Spectrosc.* **1987**, *18*, 519−523.
(28) Rimai, L.; Heyde, M. E.; Gill, D. *J. Am. Chem. Soc.* **1971**, *93*, 6776−6780.

of the free astaxanthin model corresponds closely to the experimental value for astaxanthin. As discussed above, the underestimation of the excitation energy within TDDFT is in line with previous theoretical investigations for long polyenes. Nevertheless, the shift due to a change in conformation or to the presence of hydrogen bonds is reliable.

In the s-cis-free astaxanthin model optimized within the semiempirical AM1 approach, the end rings form a dihedral angle of ~46° with the polyene chain. This is in close agreement with the 43° angle observed in X-ray studies of canthaxanthin.[29] According to the X-ray structure of β-crustacyanin,[9] the astaxanthin chromophores bound to the protein are in an all-*E* conformation with the end rings essentially coplanar to the polyene chain. Thus, the main conformational change from free astaxanthin to the chromophore in β-crustacyanin consists of the coplanarization of the end rings, thereby, inducing a more extended conjugated chain. Comparing models I and II, we find that this protein-induced conformational change produces a shift of 0.12 eV ($\Delta\lambda_{max} = 24$ nm). The next step is the inclusion of polarization effects induced by hydrogen-bonding interaction. The X-ray structure of β-crustacyanin[9] has revealed an asymmetric environment of the chromophore with a histidine and a water molecule hydrogen bonded to the keto oxygens. In model III, we include these interactions explicitly and obtain a further shift in the excitation energy, though relatively small, giving a total shift of 0.19 eV ($\Delta\lambda_{max} = 39$ nm) compared to the s-*cis*-astaxanthin model.

We have also calculated Mulliken partial atomic charge differences between models I and III. We find that the hydrogen bonds induce a small positive charge on the chromophore, which is consistent with the small positive charge difference estimated on the basis of ^{13}C chemical shift data for α-crustacyanin, thus further supporting the conclusion that keto groups are not protonated and no strong polarization occurs upon binding.

An analysis of the HOMO and LUMO orbitals for models I and III (figure available as Supporting Information) shows that a charge displacement from the center of the chromophore toward the rings occurs upon excitation in the model, including the hydrogen bonding with the protein environment, while little charge displacement is observed for the free chromophore.

We turn then our analysis on the importance of aggregation effects for the bathochromic shift mechanism. A first-order estimate of the exciton splitting induced by the proximity of the chromophores in the protein can be obtained using the dipole−dipole approximation. We use the X-ray structural information available for β-crustacyanin to evaluate the geometrical factor, and we compute the transition dipole moment within the TDDFT for model III. The two bound astaxanthins in β-crustacyanin approach each other within 7 Å at a position close to the C11−C12 bond. As can be seen in Figure 1, the long axes of the molecules form an angle of about 120°. The computed transition dipole moment is very intense (~19 D) and oriented parallel to the long axis of the molecule pointing toward the ring hydrogen bonded to the His residue. By using this information together with the orientation factor in the dipole−dipole approximation, we obtain an exciton splitting of 0.49 eV. If we add the exciton splitting to the previously computed on-site shift for model III, we obtain a $\lambda_{max} = 650$ nm (see Table 2). Even considering the limitation of the simple dipole−dipole approximation used here, we can conclude that the aggregation effects appear to give the largest contribution in determining the total bathochromic shift.

Discussion

In principle, two hypotheses could serve as a basis for understanding the bathochromic shift. The first hypothesis is exciton coupling of the transition dipole moments in the excited state, and the second hypothesis is interactions of the protein with the astaxanthin chromophore in the ground state via a polarization mechanism. The exciton coupling hypothesis was first suggested on the basis of the observed circular dichroism spectra of α- and β-crustacyanin.[1,13,30] However, the importance of this effect has been underestimated since it was expected that a strong coupling should give rise also to large changes in the shape of the absorption bands which were not observed.[1] The resonance Raman spectra of Salares et al.[4] showed a lowering in the $\nu_{C=C}$ frequency indicative of electron delocalization in the electronic ground state. On the basis of these Raman spectra, the polarization hypothesis was strongly supported and it has since become favored as the primary basis of the bathochromic shift. Moreover, it was pointed out that the argument that a large red shift in the absorption maximum should be accompanied by a change in absorption profile was not necessarily true.[4]

In view of our results from the SSNMR, Raman spectroscopy, and quantum chemical calculations, we can now evaluate these two hypotheses for the bathochromic shift in more detail. First, it should be noted that the SSNMR and Raman spectroscopy analyses are performed on α-crustacyanin, whereas the computational analysis is carried out on models based on the known structure of β-crustacyanin. We assume that the effects that are responsible for the bathochromic shift in both carotenoproteins are qualitatively comparable and that the chromophore−protein interactions are similar in α- and β-crustacyanin. This is based on the knowledge that α-crustacyanin is an aggregate of eight β-crustacyanin units and supported by the similar shape of the UV−vis, optical rotary dispersion, Raman spectra, and same sign pattern in CD spectra of α- and β-crustacyanin.[1,13]

The SSNMR experiments show that no strong polarization effect in the ground state takes place upon binding of astaxanthin in the protein. We can definitely discard now the earlier hypothesis that a large charge effect, such as protonation, near the keto groups of the chromophore is responsible for the bathochromic shift. Indeed, a strong electrostatic effect, such as the one induced by protonation, should give much larger changes in the chemical shifts of the atoms close to the ring.[24] The rather small NMR chemical shift differences (see Table 1) are indicative of small changes in the ground-state electronic distribution due to the rotation of the end rings and to polarization effects due possibly to hydrogen bonding with the protein. These conclusions are consistent with the X-ray analysis of the binding site of β-crustacyanin. Although the resolution of the X-ray data is not sufficient to determine protonation states, no charged amino acids were observed in the proximity of the astaxanthin ring.[9] Our SSNMR data show that the absence of strong polarization effects due to charged residues is true also in α-crustacyanin.

(29) Bart, J. C. J.; Macgillavry, C. H. *Acta Crystallogr. B* **1968**, *24*, 1587.

(30) Pawlikowski, M. *Acta Phys. Pol.* **1988**, *A74*, 145−149.

A comparison of the resonance Raman spectra of astaxanthin and α-crustacyanin, show that the ν_1-line, which is assigned to the C=C stretch vibration, is shifted to a lower wavenumber, consistent with previous Raman studies. The observed downshift of the ν_1-line can be correlated to the rotation around the C6−C7 bond of the chromophore from 6-s-cis to 6-s-trans. This conformational change extends the conjugated polyene, leading to a larger delocalization of the π-electron system. However, the observed shift does not quantitatively fit the empirical relationship found for carotenoids between the ν_1-vibration and $1/\lambda_{max}$.[27] This indicates that in addition to the extension of the conjugated system, other factors must contribute to the bathochromic shift.

We also observed a striking change in the spectral region near the ν_2-line of the carotenoprotein with ^{13}C labels in the chromophore at the [8,8′,9,9′,10,10′,11,11′,19,19′] (**1b**) positions where an intense band is present at 1122 cm^{-1}, while in free ^{13}C-labeled carotenoids, a weak band appears. The enhanced intensity of this band is a direct indication that the electronic excited state delocalizes upon binding to the protein, adding Raman oscillator strength to this mode.

Quantum chemical calculations on molecular models obtained from the X-ray data of β-crustacyanin show that the transition from 6-s-*cis*-astaxanthin to 6-s-*trans*- is accompanied by a considerable change in λ_{max} to 502 nm. This is by far not sufficient to account for the full bathochromic shift that occurs upon binding.[31] Also, the effect of hydrogen bonding due to the presence of a water molecule and a histidine close to the astaxanthin carbonyl gives rise to a small bathochromic shift, the combined effects shifting λ_{max} to 517 nm. Therefore, on the basis of our TDDFT calculations, we can conclude that the total protein-induced on-site effects on the bathochromic shift are not very large and can account for only about 30% of the total observed bathochromic shift in α-crustacyanin and 40% of the bathochromic shift in β-crustacyanin.

The charge displacement from the center of the chromophore toward the end rings upon excitation shown by the analysis of the HOMO and LUMO orbitals (figure available as Supporting Information) is in line with the large effect observed on the Raman ν_2-line. This charge displacement is also consistent with Stark experiments showing an enhancement in the excited-state dipole moment for α-crustacyanin compared to that of isolated astaxanthin.[32]

Our study strongly supports the hypothesis of exciton coupling as the main source of the bathochromic shift. Indeed, when we take the dipole−dipole interactions between the astaxanthin molecules in β-crustacyanin into account, a large exciton splitting is found. The exciton splitting and the angle of about 120° between the dipole moments are consistent with the negative chirality observed in CD spectra of α- and β-crustacyanin.[1−3,30] When we add the exciton coupling to the on-site effects due to the more extended conjugation and hydrogen-bonding polarization, we obtain a $\lambda_{max} \approx 650$ nm. The calculated total shift is even larger than the observed bathochromic shift. In fact, our estimate of the exciton splitting is based on the structural information on the dimer in β-crustacyanin, where $\lambda_{max} = 586$ nm. It is very likely that the simple approximation of the dipole−dipole interaction in the excited state used here overestimates the exciton splitting. Further refinement in the modeling is needed to obtain a more quantitative estimate of the exciton splitting. Nevertheless, we can clearly conclude that aggregation effects give the largest contribution to the observed color shift.

The bathochromic shift in α-crustacyanin is larger than that in β-crustacyanin ($\lambda_{max} = 632$ and 586 nm, respectively). The X-ray analysis of β-crustacyanin suggests that subunit−subunit interaction can take place in the aggregation of eight dimers in α-crustacyanin.[9] This interaction could induce a larger exciton splitting in α-crustacyanin, though a proper description of this effect needs further investigation.

Conclusions

We have explored the coloration mechanism of astaxanthin in α-crustacyanin by using solid-state NMR and resonance Raman spectroscopy complemented by quantum chemical calculations based on time-dependent DFT. Solid-state NMR spectra of the ^{13}C-enriched α-crustacyanin show that only minor changes in the ground-state electron density of astaxanthin occur upon binding, thus ruling out the hypothesis of a strong polarization. From the comparison of Raman spectra for ^{13}C-labeled astaxanthin and α-crustacyanin, we conclude that delocalization of the electronic excited state of the polyene chain close to the ring occurs upon binding. Time-dependent DFT calculations show that the protein-induced conformational changes and polarization effects contribute to about 30% of the total bathochromic shift in α-crustacyanin. The exciton coupling due to the proximity of the astaxanthin chromophores, estimated using the β-crustacyanin dimer structure, is found to be large and can account for the additional absorption shift.

Acknowledgment. The authors are grateful to C. Erkelens, J. Hollander, and F. Lefeber for support with the NMR experiments. G. Britton, D. Philips, P. Gast, and J. Brouwer have been involved in the protein isolation and purification. The sample of $^{13}C_{10}$ β,β-carotene was kindly provided by M.A. Verhoeven. F.B. acknowledges T. Aartsma for useful discussions. The 750 MHz NMR equipment was financed in part by Demonstration Project Grant BIO4-CT97-2101 (DG12-SSMI) of the commission of the European Communities.

Supporting Information Available: ^1H and ^{13}C NMR characterizations of ^{13}C-labeled astaxanthins **2a** and **2b**; coordinates and figures of HOMO and LUMO orbitals of 6-s-*cis*-astaxanthin (I) and 6-s-*trans*-astaxanthin, including a hydrogen-bonded histidine analogue and a water molecule (III). This material is available free of charge via the Internet at http://pubs.acs.org.

JA045049+

(31) Durjeeb, B.; Eriksson, L. A. *Chem. Phys Lett.* **2003**, *375*, 30−38.
(32) Krawczyk, S.; Britton, G. *Biochim. Biophys. Acta* **2001**, *1544*, 301−310.